Dynamics of the Type III Secretion System Activity of Enteropathogenic *Escherichia coli*

Erez Mills,[a] Kobi Baruch,[a] Gili Aviv,[a] Mor Nitzan,[a,b] Ilan Rosenshine[a]

Department of Microbiology and Molecular Genetics, Institute of Medical Research Israel-Canada, Faculty of Medicine,[a] and Racah Institute of Physics,[b] the Hebrew University of Jerusalem, Jerusalem, Israel

E.M. and K.B. contributed equally to this article.

ABSTRACT **Type III secretion systems (TTSSs) are employed by pathogens to translocate host cells with effector proteins, which are crucial for virulence. The dynamics of effector translocation, behavior of the translocating bacteria, translocation temporal order, and relative amounts of each of the translocated effectors are all poorly characterized. To address these issues, we developed a microscopy-based assay that tracks effector translocation. We used this assay alongside a previously described real-time population-based translocation assay, focusing mainly on enteropathogenic *Escherichia coli* (EPEC) and partly comparing it to *Salmonella*. We found that the two pathogens exhibit different translocation behaviors: in EPEC, a subpopulation that formed microcolonies carried out most of the translocation activity, while *Salmonella* executed protein translocation as planktonic bacteria. We also noted variability in host cell susceptibility, with some cells highly resistant to translocation. We next extended the study to determine the translocation dynamics of twenty EPEC effectors and found that all exhibited distinct levels of translocation efficiency. Further, we mapped the global effects of key TTSS-related components on TTSS activity. Our results provide a comprehensive description of the dynamics of the TTSS activity of EPEC and new insights into the mechanisms that control the dynamics.**

IMPORTANCE **EPEC and the closely related enterohemorrhagic *Escherichia coli* (EHEC) represent a global public health problem. New strategies to combat EPEC and EHEC infections are needed, and development of such strategies requires better understanding of their virulence machinery. The TTSS is a critical virulence mechanism employed by these pathogens, and by others, including *Salmonella*. In this study, we aimed at elucidating new aspects of TTSS function. The results obtained provide a comprehensive description of the dynamics of TTSS activity of EPEC and new insights into the mechanisms that control these changes. This knowledge sets the stage for further analysis of the system and may accelerate the development of new ways to treat EPEC and EHEC infections. Further, the newly described microscopy-based assay can be readily adapted to study the dynamics of TTSS activity in other pathogens.**

Received 9 May 2013 **Accepted** 9 July 2013 **Published** 30 July 2013

Citation Mills E, Baruch K, Aviv G, Nitzan M, Rosenshine I. 2013. Dynamics of the type III secretion system activity of enteropathogenic *E. coli*. mBio 4(4):e00303-13. doi:10.1128/mBio.00303-13.

Editor Howard Shuman, University of Chicago

Address correspondence to Ilan Rosenshine, ilanr@ekmd.huji.ac.il.

Type III secretion systems (TTSSs) are utilized by many pathogenic bacteria, including enteropathogenic *Escherichia coli* (EPEC) and *Salmonella enterica* serovar Typhimurium, to translocate effector proteins into eukaryotic host cells (1, 2). The translocated effectors subvert normal host cell functions to the benefit of the colonizing bacteria (3). Under infection conditions, EPEC induces expression of a TTSS and of type 4 pili termed bundle-forming pili (BFP) and represses expression of flagella (4, 5). Upon BFP expression, an EPEC subpopulation aggregates to form microcolonies, each composed of a few dozen bacteria. Microcolony formation enhances EPEC attachment to the host cell and promotes the activity of the TTSS (6). The attached EPEC delivers a battery of effectors, including Tir, which is inserted into the host cell membrane, and forms a binding site for the bacterial outer membrane protein intimin, leading to intimate attachment of EPEC to the host cell (7). The attached EPEC remains extracellular and from this location continues to modulate host cell processes. This modulation requires intimin, Tir, and additional effectors, six of which are encoded on the conserved locus of enterocyte effacement (LEE), which also encodes TTSS components, dedicated chaperones, and regulators (8). Additional effectors are encoded at several chromosomal locations, and their total number in different isolates ranges from 16 to over 40 (reviewed in reference 7).

Salmonella Typhimurium possesses two TTSSs encoded in *Salmonella* pathogenicity islands 1 and 2 (SPI-1 and SPI-2). Under infection-inducing conditions, *Salmonella* Typhimurium expresses both SPI-1 and flagella and attacks the intestinal epithelium as a motile planktonic bacterium (9). Upon contact with intestinal epithelial cells, it employs the SPI-1 TTSS to translocate into host cells a set of effectors, including SopE and SptP, which mediate rapid membrane remodeling associated with bacterial in-

vasion into nonphagocytic host cells (10). The SPI-2 TTSS is required for survival of *Salmonella* Typhimurium in macrophages and for systemic spread (10).

TTSS effector proteins typically contain two dedicated domains recognized by the TTSS machinery: the N-terminal signal domain spanning the first ~25 residues of an effector and the chaperone-binding domain located downstream from the N-terminal signal domain. Dedicated TTSS chaperones bind to the chaperone-binding domain and promote effector translocation via diverse mechanisms, including effector stabilization, maintenance of effectors in a secretion-competent conformation, and targeting of bound effectors to the translocation apparatus (summarized in reference 11). Two TTSS effector chaperones have been identified in EPEC: CesF and CesT. CesF is required for EspF translocation, while CesT is required for translocation of several effectors, including EspH, Map, Tir, EspZ, NleA, NleF, NleG, NleH1, and NleH2 (6, 12–18). By promoting secretion of specific effectors, CesT and CesF are involved in establishing a secretion hierarchy. Tir secretion was also reported to be required for the efficient secretion of additional effectors and thus is necessary for establishing the secretion hierarchy (18).

In a previous study, we described the translocation dynamics of the six LEE effectors using an assay that allows parallel quantitative analysis of multiple translocation events in real time (6). The assay involves infection of host cells prelabeled with CCF2, a caged β-lactamase substrate composed of two fluorophores linked by a β-lactamic ring. The method utilizes bacteria expressing effectors fused at their C terminus to β-lactamase (BlaM). Upon translocation, the effector BlaM catalyzes CCF2 hydrolysis, thus disrupting Förster (fluorescence) resonance energy transfer (FRET) between the two fluorophores, generating a dynamic fluorescence shift that can be traced by a fluorometer. Using this approach, we demonstrated that each of the six LEE effectors is translocated with a different level of efficiency. While this method allows measuring the average dynamics of effector translocation, it cannot resolve the distribution of events within the population. For example, it is not clear whether protein translocation into the host cell is carried out by a specific EPEC subpopulation. It is also unknown if attachment and translocation into host cells occur simultaneously. Another unresolved issue is whether the behavior of the six LEE effectors reflects that of the entire cohort of EPEC effectors or, alternatively, whether the translocation of non-LEE effectors is regulated differently from that of LEE effectors.

The aim of this study was to address these unresolved issues. To tackle the first issue, we developed a time-lapse microcopy translocation assay which allows single-cell analysis and thus probes the distribution of events within the population. We used this assay for single-cell analysis of Tir translocation mediated by EPEC and compared it with that performed by *Salmonella* Typhimurium. To investigate the second issue, i.e., the translocation dynamics of non-LEE effectors, we used a population-based assay to achieve simultaneous analysis of the translocations of twenty EPEC effectors, including most of the non-LEE effectors. This analysis was carried out using wild-type EPEC as well as EPEC mutated in key factors involved in setting the translocation hierarchy. Our results provide a comprehensive description of the dynamics of the TTSS activity of EPEC.

RESULTS

Time-lapse-microscopy analysis of Tir translocation by EPEC. We developed a time-lapse-microscopy translocation assay based on CCF2 and the *blaM* reporter gene to visualize protein translocation by EPEC. To this end, HeLa cells preloaded with CCF2 were inoculated with EPEC harboring a chromosomal *tir-blaM* protein fusion (strain CX2135) and an mCherry-expressing plasmid (pKB4985). The infection was monitored by time-lapse microscopy at 90-s intervals. We recorded the behavior of the infecting bacteria (red channel) and the host cells (phase contrast). We also recorded the rate of CCF2 hydrolysis (green and blue channels), which is in direct correlation with the amount of translocated Tir-BlaM. As expected, some of the bacteria aggregated to form microcolonies, while the other portion of the culture remained planktonic (see Movie S1 in the supplemental material). The microcolonies exhibited rapid and robust interaction with the host cells, and, following attachment, these colonies assumed a flatter shape and increased in size. Size increase was mediated by both cell division and recruitment of additional microcolonies (Fig. 1A and Movie S2).

To determine the relationship between microcolony attachment and protein translocation, we carried out a detailed analysis of the infection process of 11 specific host cells. For each host cell, we recorded the time points of microcolony attachment as well as the rate of CCF2 hydrolysis. The attachment of the first and second microcolonies occurred at between 15 and 105 min and between 50 and 130 min postinoculation, respectively (Fig. 1B). For each cell, we established the time point at which the amount of the product generated by CCF2 hydrolysis reached 50% of its maximal level ($t_{50\%}$), a value which correlates with the time point of translocation initiation and amount of translocated effector. Next, we calculated the correlation coefficients of the attachment time points for the first and second microcolonies versus the $t_{50\%}$ and found them to be 0.75 and 0.53, respectively. These results suggest that most of the translocated Tir was contributed by the pioneering microcolony.

Variability in translocation efficiency. To evaluate variability among host cells in the rate of CCF2 hydrolysis, we normalized the data shown in Fig. 1B by setting the attachment time of the first microcolony as zero (0.0 min) and by expressing the rate of CCF2 hydrolysis using values ranging from zero to one (Fig. 1C). Notably, some microcolonies initiated Tir-BlaM translocation immediately upon attachment, while others exhibited a lapse of up to 30 min between attachment and initiation of translocation (pausing time). One source of the variability in pausing time is likely related to features of the involved microcolony, such as microcolony size. Another possible source of variability is individual host cell characteristics. In support of this notion, we found that while the vast majority of cells were translocated into within less than 150 min postinoculation, some cells remained immune to bacterial attachment and were not translocated in a detectable manner at even 180 min postinoculation. Interestingly, translocation-resistant cells frequently exhibited a transient membrane blebbing phenotype at some point during the infection assay (Fig. 1D; see aslo Movie S3 in the supplemental material). In conclusion, our results demonstrate that EPEC microcolonies exhibit an intriguing lapse between attachment and initiation of translocation. Furthermore, a striking variability in the efficiency of Tir translocation into different host cells was evident.

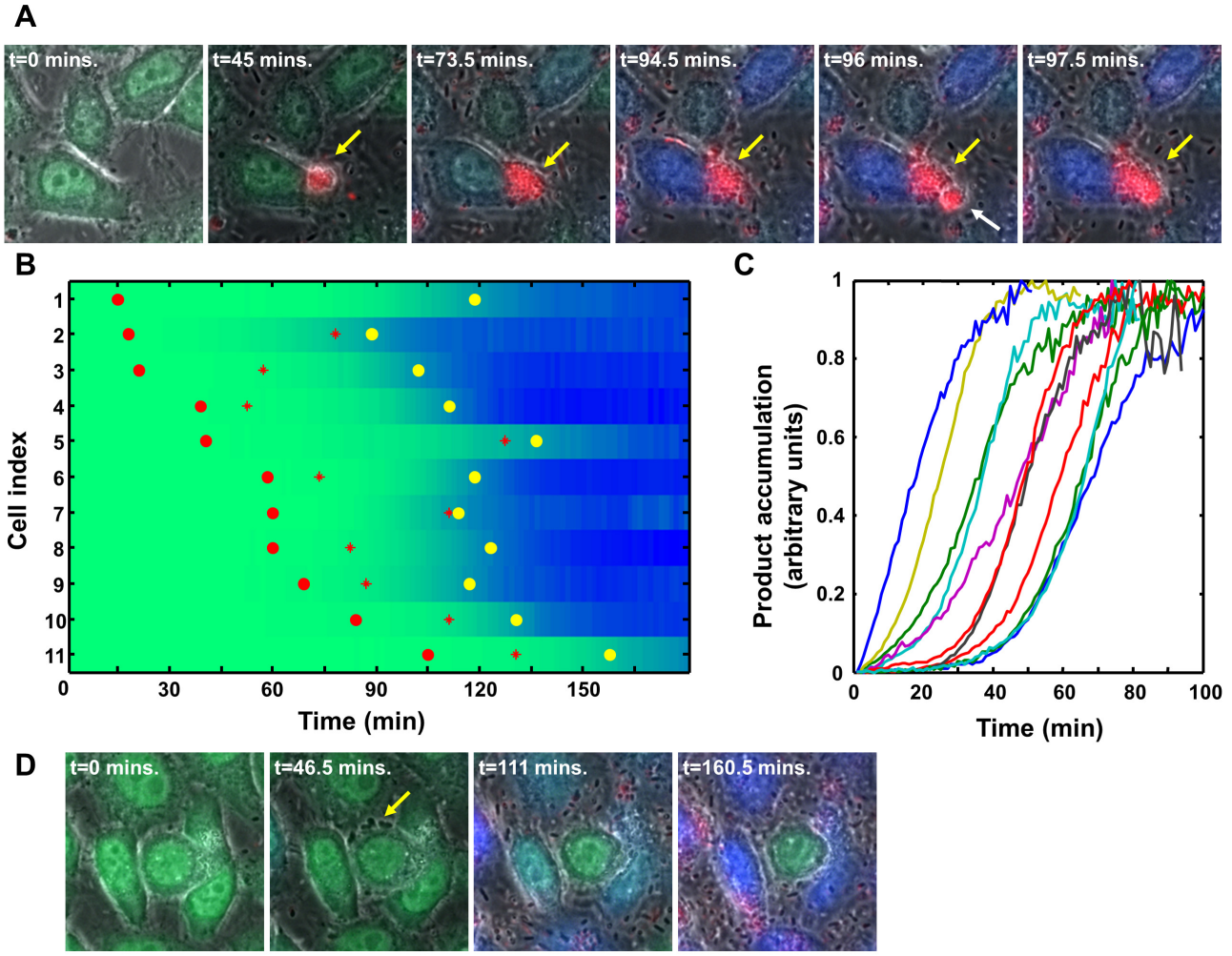

FIG 1 Single-cell imaging of Tir translocation by EPEC. HeLa cells preloaded with CCF2 were infected with EPEC expressing Tir-BlaM from the native promoter and mCherry as a bacterial marker. Infection was carried out under the microscope, and images were captured using phase-contrast, green channel (intact CCF2), blue channel (hydrolyzed CCF2), and red channel (bacteria) microscopy for 3 h at 90-s intervals. (A) Selected frames taken from Movie S2 in the supplemental material. The respective time points postinfection are indicated above each frame. A pioneering microcolony is indicated by the yellow arrow, and the white arrow indicates a recruited microcolony. (B) Translocation dynamics of 11 HeLa cells. The raw data are represented by the shift from green (substrate) to blue (product). Yellow dots indicate 50% of maximal product accumulation level, red dots indicate attachment time of the pioneering microcolony, and red asterisks indicate attachment time of a second or recruited microcolony (where it existed). (C) Plot of the dynamics of translocation into the 11 cells shown in panel B. The data were normalized using the attachment time of the pioneering microcolony as t_0. Translocation levels are presented using a scale of 0.0 to 1.0. (D) Selected frames taken from Movie S3. The respective time points postinfection are indicated above each frame. Yellow arrows indicate blebbing buds generated by a cell resistant to translocation.

Individual *Salmonella* Typhimurium bacteria effectively translocate effectors into host cells. While EPEC depends on microcolony formation for efficient protein translocation, *Salmonella* Typhimurium executes protein translocation as a planktonic bacterium. Thus, we decided to examine the process of protein translocation by *Salmonella enterica* serovar Typhimurium (strain SL1344) and to compare it to that of EPEC. Chromosomal *blaM* fusions with several SPI-1 TTSS *Salmonella* Typhimurium effector genes were constructed, and conditions for the translocation assay were optimized (see Fig. S1 in the supplemental material). Next, we tracked translocation carried out by *Salmonella* Typhimurium expressing *sptP-blaM* (strain KB3169). Phase-contrast microscopy was used to visualize the cells and infecting bacteria and the green and blue channels to monitor CCF2 hydrolysis. In contrast to EPEC, tagging *Salmonella* Typhimurium with plasmids expressing fluorescent proteins interferes with the translocation process (see Fig. S1) and therefore could not be used to determine the time of initial bacterium-host cell contact. Instead, we used formation of membrane ruffles as a marker for host cell contact and translocation initiation. Formation of membrane ruffles is dependent on SopE translocation and was reported to appear ~1 min posttranslocation initiation (19, 20). To increase the chances that each *Salmonella* Typhimurium-host cell encounter involves only a single bacterium, we minimized the multiplicity of infection (MOI) to an effective value of approximately 1 (see Fig. S2 and Materials and Methods).

The infecting *Salmonella* Typhimurium bacteria were planktonic and highly mobile and induced membrane ruffles followed

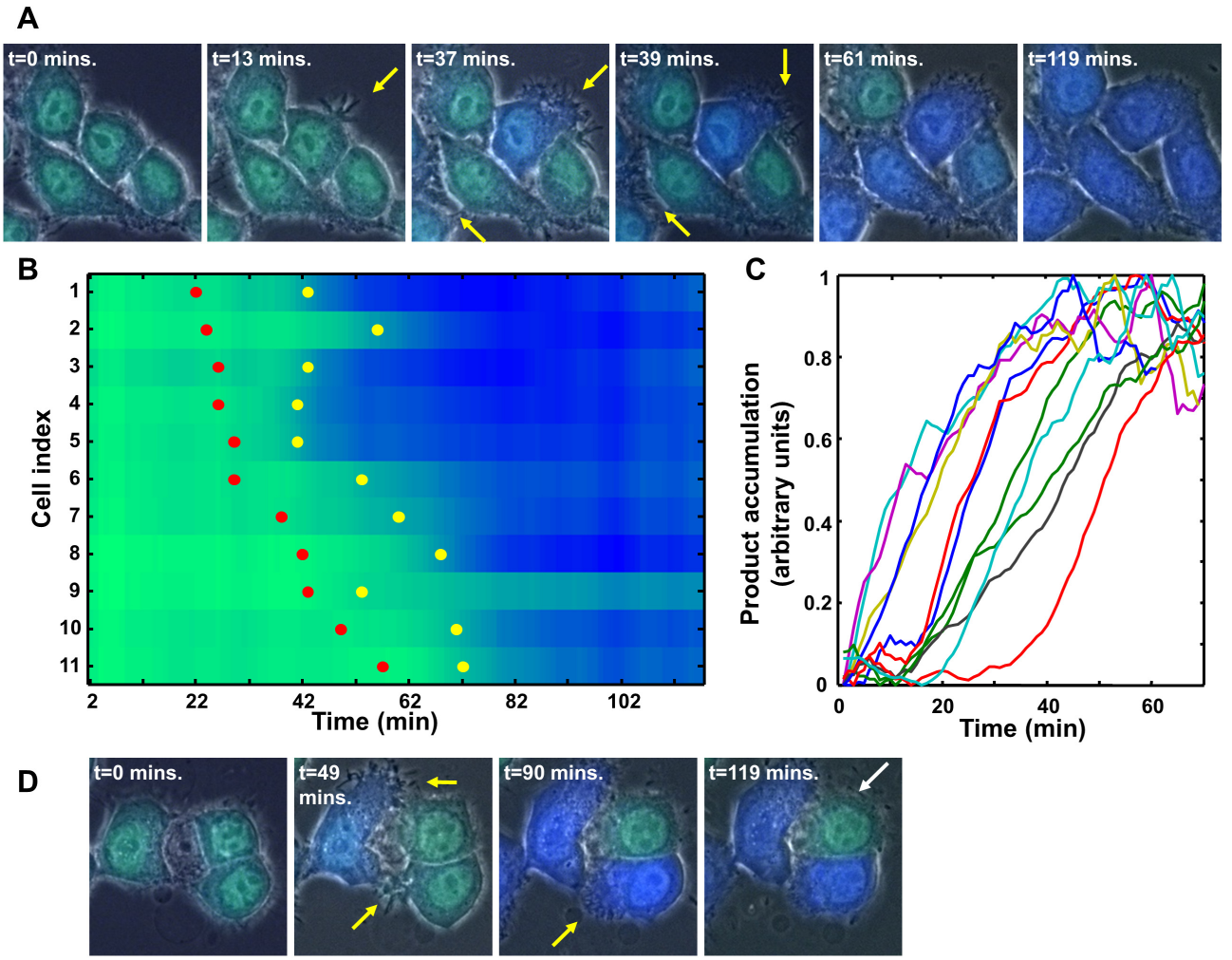

FIG 2 Single-cell imaging of SptP translocation by *Salmonella* Typhimurium. HeLa cells preloaded with CCF2 were infected with *Salmonella* Typhimurium expressing SptP-BlaM via the native chromosomal location. Infection was carried out in a temperature-controlled automated microscope, and images were captured at 1-min intervals for 2 h using phase-contrast, green channel (intact CCF2), and blue channel (hydrolyzed CCF2) microscopy. (A) Selected frames taken from Movie S4 in the supplemental material. The respective time points postinfection are indicated above each frame. Membrane ruffles are indicated by yellow arrows. (B) Translocation dynamics of 11 HeLa cells. The raw data are presented by the shift from green (substrate) to blue (product). Yellow dots indicate 50% of maximal product accumulation level, and red dots indicate the time point of initial appearance of ruffles on the analyzed cell. (C) Plot of the dynamics of translocation into the 11 cells shown in panel B. The data were normalized using the ruffle appearance time as t_0. Translocation levels are presented using a scale of 0.0 to 1.0. (D) Selected frames taken from Movie S5. The respective time points postinfection are indicated above each frame. Membrane ruffles are indicated by yellow arrows, and a white arrow points to a cell resistant to translocation.

by rapid CCF2 hydrolysis (Fig. 2A; see also Movie S4 in the supplemental material). Analysis of 11 infected cells showed that the ruffle appearance time ranged between host cells from 19 to 55 min postinoculation (Fig. 2B and C) and correlated well with translocation dynamics (correlation coefficient of ruffle appearance time versus $t_{50\%}$ = 0.85). Maximal product accumulation levels were reached between 65 and 100 min in the different infected cells. Similar results were obtained using strains expressing SopE2 or SopE BlaM chromosomal protein fusions (KB3370 and KB3496; data not shown). Interestingly, the efficiency of SptP translocation by a single *Salmonella* Typhimurium bacterium was comparable to that of Tir translocation mediated by an entire EPEC microcolony (compare Fig. 1B to Fig. 2B). As observed during an EPEC infection, we found that some cells remained immune to *Salmonella* Typhimurium translocation. In these cells, neither *Salmonella* Typhimurium-induced ruffles nor CCF2 hydrolysis was evident even 120 min postinoculation (Fig. 2D; see also Movie S5). Taken together, our results show that single *Salmonella* Typhimurium bacteria exhibit translocation efficiency equal to that mediated by an entire EPEC microcolony but show lesser variability in the efficiency of effector translocation into different host cells. This variability is mediated by host cell characteristics and possibly by variability in traits related to individual bacteria.

Translocation dynamics of 20 EPEC effectors. We next extended our study to analyze the translocation dynamics of 20 of the 22 known effectors of the EPEC E2348/69 strain (3, 7, 21). We constructed 20 EPEC strains with each containing a different effector gene fused to *blaM* as a chromosomal fusion expressed from the native promoter. Testing translocation dynamics of 20 effec-

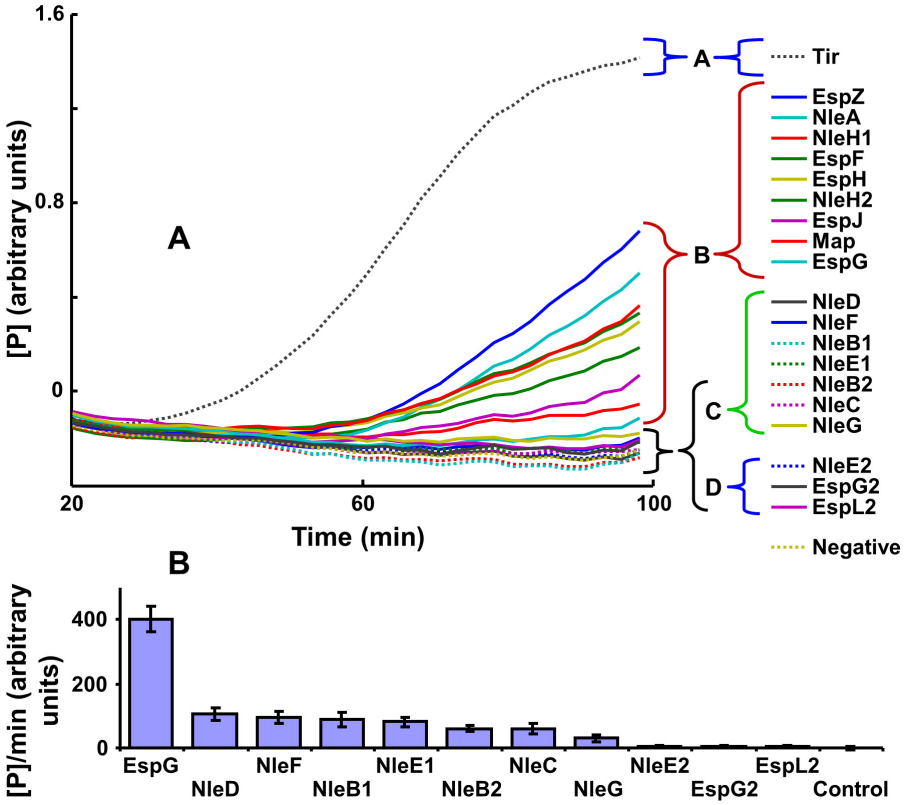

FIG 3 Translocation dynamics of EPEC effectors. (A) EPEC strains, each containing a different chromosomally encoded effector-BlaM gene, were subjected to real-time translocation analysis. The results of a typical experiment of three conducted are shown. Each data point represents the average of triplicate results. EPEC that does not carry a BlaM fusion was used as a negative control. On the right, effectors are listed from the most efficiently translocated (Tir; top) to the least efficiently translocated, and clustering of effectors into groups A to D is indicated. Error bars are omitted for clarity. (B) EPEC strains, carrying chromosomal effector-BlaM genes encoding effectors whose translocation could not be detected by the real-time translocation assay, were subjected to the more sensitive STPT assay. The results of a typical experiment are shown. Each data point represents the average of quadruplicate results. An EPEC strain that does not carry a BlaM fusion was used as a negative control. An EPEC strain carrying chromosomal *espG-blaM* was used as a reference for comparisons between panels A and B. The bars represent standard deviations.

tors by microscopy is technically challenging, and we thus adopted the population-based assay for this task. Of note, averaging the signal created by the 11 host cells infected with EPEC produced a pattern resembling that observed by the population-based assay (Fig. S2), indicating that the results obtained by population-based analysis and single-cell analysis are in agreement. We found that translocation of some effectors could not be detected by the real-time translocation assay. Thus, translocation of these effectors was further analyzed by the more sensitive single-time-point translocation (STPT) assay (see Materials and Methods). The results showed that all effectors exhibited distinct kinetics of effector translocation and/or reached different maximal levels in the host cells (Fig. 3).

The maximal levels of effectors in the host cells were measured over a range greater than 50-fold, with Tir exhibiting the highest abundance whereas the NleE2, EspL2, and EspG2 levels were below the detection level. The effectors clustered into four groups, according to their translocation efficiency. Group A includes only Tir. Group B consists of effectors translocated at an efficiency that allowed detection using the real-time translocation assay and includes five LEE and four none-LEE effectors (Fig. 3). The translocation of chromosomally encoded group C effectors could be detected only by the more sensitive STPT assay (Fig. 3B). Group D effectors consisted of EspG2, EspL2, and NleE2, whose translocation could be detected only upon expression from a plasmid (see the supplemental material). These results demonstrate that the EPEC effectors exhibit distinct translocation efficiencies, constituting together a wide spectrum of efficiencies, with a more than 50-fold difference between the translocation efficiencies of the Tir and group D effectors.

Tir absence has divergent effects on the translocation of effectors. Tir is inserted into the host cell membrane shortly after translocation, forming a binding site for the EPEC outer membrane protein intimin and thus promoting intimate bacterial adherence (22). It has been suggested that translocation of other effectors depends upon earlier Tir translocation to form a translocation hierarchy (18, 23, 24). In agreement with these studies, we found that Tir is clearly the first effector to be translocated (Fig. 3). To test how Tir affects translocation of other effectors, we inserted the 20 effector-*blaM* fusions into the chromosome of a *tir* mutant and compared the translocation by this mutant to that exhibited by wild-type EPEC. Group B effectors were compared by real-time translocation assays and group C effectors by STPT assays. Notably, all the tested effectors were translocated in the absence of Tir, indicating that Tir is not essential for translocation of other effectors (Fig. 4; see also Fig. S3 in the supplemental ma-

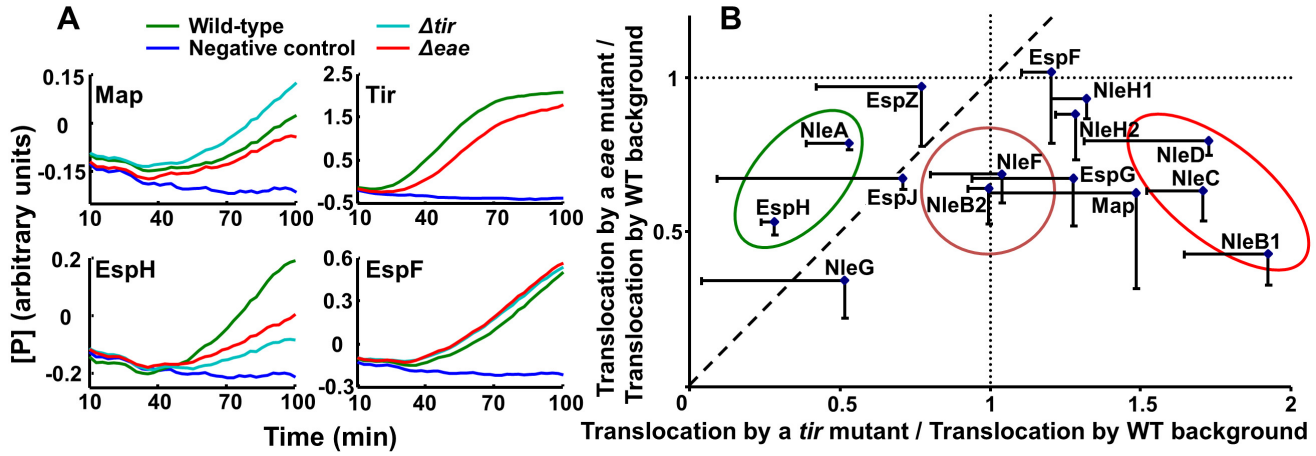

FIG 4 Effector translocation in the absence of Tir or intimin. Wild-type EPEC and mutants in either *tir* or *eae* carrying effector-BlaM fusion genes were used for real-time or STPT assays. (A) Translocation dynamics of Map, EspH, Tir, and EspF, representing different effector types, are shown. Each data point represents the average of quadruplicate results. Dark blue represents the negative control. Tir translocation was not studied in the Δ*tir* background. Typical results of one experiment of three are shown. Results related to the other effectors are shown in Fig. S3 in the supplemental material. Error bars are omitted for clarity. (B) Effector translocation by the *eae* and *tir* mutants. The average results from at least three experiments, each conducted in duplicate or quadruplicate, are shown as ratios of translocation in the mutant to that in the wild type (WT). A ratio of 1 indicates that translocation by the mutant was similar to that exhibited by wild-type EPEC. The two dotted lines indicate the numerical value of 1. The dashed diagonal line shows the values corresponding to equal levels of effector translocation in the *tir* and *eae* backgrounds. The differences in translocation between the effectors marked by ovals were statistically significant: $P < 0.02$ for the effectors in the green oval compared to the brown, $P < 0.04$ for the effectors in the brown oval compared to the red, and $P < 0.01$ for the effectors in the green oval compared to the red. The bars represent standard deviations.

terial). However, the absence of Tir influenced the efficiency of effector translocation. For instance, translocation of EspH and NleA was reduced by ~1.5-fold and that of NleB1, NleC, and NleD was increased by 1.5- to 2-fold (Fig. 4 and Fig. S3).

Intimin absence results in a moderate reduction in translocation efficiency. The shifts in the translocation rates in the absence of Tir might result from the inability of EPEC to form an intimate attachment. To test this hypothesis, we examined whether the absence of intimin would influence effector translocation in a similar way. An *eae* mutant was used to generate strains containing chromosomal effector-*blaM* fusions, and protein translocation mediated by these strains was compared to that exhibited by wild-type EPEC and by the *tir* mutant (Fig. 4; see also Fig. S3 in the supplemental material). Translocation of Tir, EspF, and EspZ was not affected by the absence of intimin, while that of other effectors was reduced by up to 60%. These results suggest that the shifts in translocation efficiencies noted in the *tir* mutant are not merely the consequence of the lack of Tir-intimin interaction. The data also indicate that intimate attachment enhances translocation of some effectors, mostly those belonging to the group exhibiting lower translocation efficiency (Fig. 3). Taken together, these results suggest that Tir and intimin have a significant, though not prominent, role in setting translocation efficiencies.

The role of chaperones in translocation of EPEC effectors. CesT and CesF are chaperones required for efficient translocation of some effectors (6, 12–18). To examine their global effect on translocation dynamics, we inserted effector-BlaM fusion genes into the chromosomes of EPEC *cesT* and *cesF* mutants and compared the translocation by these mutants to that exhibited by wild-type EPEC (Fig. 5). As before, the Tir and group B effectors were analyzed by real-time translocation assays and group C effectors by STPT assays. Translocation of only one effector, EspF, was dependent on CesF (Fig. 5A). In the case of CesT, a more complex picture emerged: translocation of Map, EspH, EspJ, EspZ, NleG, NleH1, and NleH2 was reduced dramatically to less than 10% of that of the wild-type strain, while translocation of NleA, NleB1, NleB2, NleC, and Tir was reduced only partially (Fig. 5; see also Fig. S4 in the supplemental material). Translocation of EspG, NleD, and NleF was not dependent on CesT or CesF (Fig. 5). These results show that CesT has a wide range of impact on effector translocation, extending from no impact to strict CesT dependency.

CesT and CesF are not interchangeable for translocation of Tir, NleA, and EspG. EspG is equally translocated by *cesT* and *cesF* mutants, and thus it is possible that CesT and CesF have redundant functions in EspG translocation. This suggestion is supported by a reported EspG-CesT interaction (18). Redundancy of CesT and CesF function may also account for the partial Tir and NleA dependency on CesT for translocation (Fig. 5). To test this hypothesis, we created a mutant lacking both *cesF* and *cesT* and used it to construct chromosomal *blaM* fusions of *tir*, *nleA*, and *espG*. We then compared the translocation of NleA, EspG, and Tir by the *cesT cesF* double mutant with that mediated by the *cesT* single mutant (Fig. 5A; see also Fig. S4A in the supplemental material). We found that the translocation results for all three effectors were similar in the double and single mutants. Thus, we concluded that CesT and CesF are not interchangeable for translocation of Tir, NleA, and EspG.

DISCUSSION

We previously used the BlaM reporter system (25) to study the dynamics of translocation of the six LEE effectors (6). That study provided important data on the average translocation dynamics, but the distribution of translocation events within the population remained elusive. To address this issue, we modified the assay to

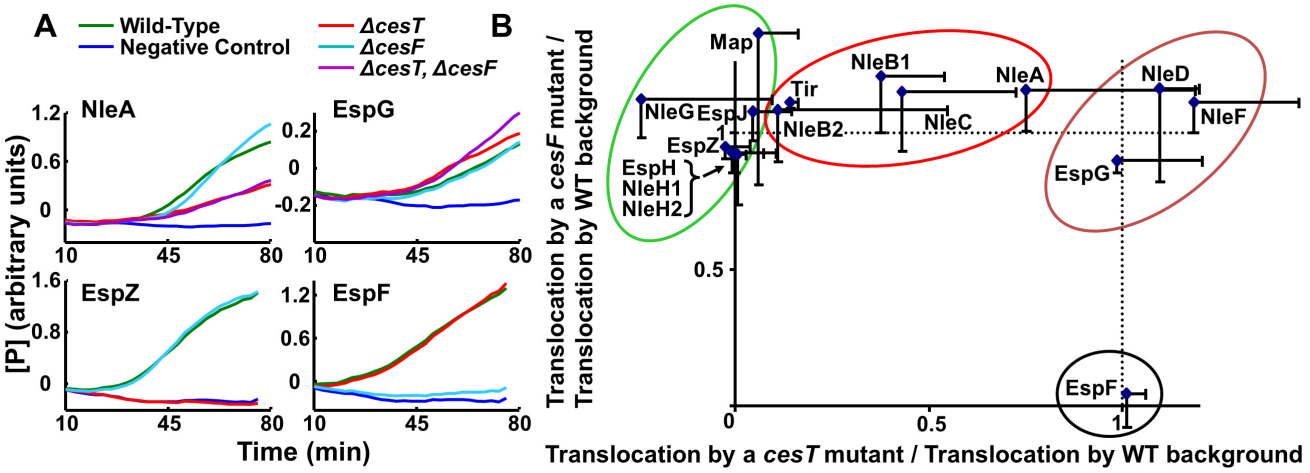

FIG 5 Effector translocation in the absence of CesT or CesF or both. (A) Translocation of strains carrying effector-BlaM fusions genes was analyzed. The results of an experiment representative of three are shown. The mutants used are indicated. Each data point represents the average of quadruplicate results. The translocation dynamics of NleA, EspG, EspZ, and EspF, which represent four distinct behaviors, are presented. Translocation of EspZ and EspF by the Δ*cesT* Δ*cesF* double mutant was not tested. Results relating to the other effectors are shown in Fig. S4 in the supplemental material. Error bars are omitted for clarity. (B) The ratio of translocation by wild-type EPEC to that by the *cesT* and *cesF* mutants was determined. The average results of at least three experiments, each of which was conducted in duplicate or quadruplicate, are shown. The two dotted lines indicate a ratio of 1, indicating that translocation by a given mutant was similar to translocation by wild-type EPEC. The bars signify standard deviations.

visualize the translocation process by time-resolved microscopy. This strategy allows direct comparison between the population-based and single-cell analyses and is adaptable for different pathogens, as exemplified here with the direct comparison between EPEC and *Salmonella* Typhimurium. The single-cell microscopic analysis provided several new insights into details that could not be detected by the population-based assay. Our data confirm that the EPEC population during infection consists of both planktonic bacteria and microcolonies. We further show that the microcolonies, which pioneer attachment to the host cells, mediate most of the protein translocation. The contribution of the microcolonies that were second to attach was lower, possibly reflecting limitations of the assay. Alternatively, this observation might support the notion of a translocation negative-feedback loop (26). The contribution of planktonic EPEC to protein translocation was small, possibly due to low levels of BFP and/or TTSS expression. Our findings, together with previous reports, indicate that BFP promote protein translocation by promoting microcolony attachment to the host cell and by BFP retraction (27, 28).

In contrast to EPEC, the entire *Salmonella* Typhimurium population remains planktonic and motile during infection. The BlaM-based time-resolved analysis allowed direct and quantitative comparison between the translocation efficiencies of Tir by EPEC and of SptP by *Salmonella* Typhimurium. The most surprising outcome of this comparison is that protein translocation by a single *Salmonella* Typhimurium bacterium is equivalent to the translocation executed by an entire EPEC microcolony containing a few dozen bacteria. This observation might reflect differences in the average numbers of TTSS apparatuses per bacterium in *Salmonella* Typhimurium and EPEC, which are ~100 and ~10, respectively (29, 30). Additionally, it is possible that only a few of the microcolony members that are in direct contact with the host cell are actively engaged in protein translocation. Finally, time-lapse microscopy highlights the existence of a small subpopulation of host cells that remained untranslocated through the infection process. What make these cells resistant to translocation by EPEC or *Salmonella* Typhimurium is currently not clear.

We next extended the study using population-based assays to determine the translocation hierarchy of 20 EPEC effectors. We found a temporal translocation order and a wide spectrum of translocation efficiencies. Importantly, in all cases, translocation efficiency directly correlated with the temporal order and none of the EPEC effectors exhibited switch behavior, i.e., a late onset of translocation with translocation efficiency higher than that of earlier effectors (Fig. 3). Thus, differences in translocation efficiency *per se* provide a mechanistic explanation for the observed temporal order of translocation. We concluded that translocation efficiency is a key factor that controls both the amount of translocated effector and the timing of translocation. The data also showed that the LEE-encoded effectors were translocated at a higher efficiency than most non-LEE effectors. It could be speculated that this may be a result of incomplete integration of relatively newly acquired non-LEE effectors with the EPEC TTSS.

Our results show that Tir is the first effector to be translocated and that it is translocated at a greater rate than all the other effectors. This suggests that the most urgent task of EPEC, upon engagement with the host cell, is to establish an intimate attachment which is mediated by Tir-intimin interaction. We examined whether Tir and intimin similarly influence translocation dynamics. The data show that the EPEC *eae* mutant mediated normal translocation of effectors exhibiting high translocation efficacy and that translocation of effectors that exhibit lower translocation efficiency was somewhat attenuated. Thus, intimin has a modest positive effect on translocation of late effectors. In contrast, absence of Tir caused diverse effects on translocation efficiency: some effectors were positively affected, while others were negatively affected. The observed shifts, although significant, were not dramatic. Interestingly, however, in some cases effectors that have opposite biological functions were also inversely influenced by the lack of Tir. For example, Map and EspH maintain a delicate bal-

ance; EspH is an inhibitor of a GTPase exchange factor (GEF) that intoxicates the cells, while Map neutralizes EspH's toxicity via its GEF activity (31). Notably, we found that the absence of Tir resulted in an increase in Map translocation and a decrease in EspH translocation, possibly disrupting the delicate balance between their GEF and anti-GEF activities. These data may provide new interpretations of previous observations that deletion of either *tir* or *espH* resulted in an increase in Map GEF activity (32, 33).

The global effect of CesT and CesF on effector translocation was also tested. Our results show that lack of CesF reduced the translocation of only one effector, EspF. In contrast, lack of CesT caused reduced translocation of 12 effectors to various degrees ranging from a very partial to a drastic translocation reduction. Next, using a *cesT cesF* double mutant, we ruled out the possibility that for some effectors both CesT and CesF promote translocation. Thus, the translocation of NleD, NleF, and EspG is CesF and CesT independent. It is not known if their translocation is chaperone independent or if a third effector chaperone exists. To summarize, these results highlight the complex role of the chaperones, and particularly that of CesT, in controlling the relative translocation efficiencies of different effectors.

MATERIALS AND METHODS

Primers, strains, and plasmids. Strains, plasmids, and primers used in this study are listed in Table S1, Table S2, and Table S3, respectively. Mutants and plasmid and chromosomal effector-*blaM* fusions were constructed using standard procedures (a full description can be found in Text S1 in the supplemental material).

Population-based real-time translocation assays. Real time translocation assays were performed as previously described (6).

Population-based STPT assay. The single-time-point translation (STPT) assay was performed as follows. HeLa cells were seeded in 96-well plates (Greiner Bio-One) (black with clear bottom) at a density of ~2 × 10^4 cells/well in Dulbecco's modified Eagle's medium (DMEM) (Sigma) supplemented with 10% fetal calf serum (FCS) and antibiotics (penicillin-streptomycin [Pen/Strep]). In parallel, bacterial strains were inoculated and grown overnight in LB broth, at 37°C, as a static culture. The next day, the HeLa cells were washed twice with phosphate-buffered saline (PBS), overlaid with 200 μl of DMEM, and infected with 5 μl of an EPEC overnight culture. The infected cells were incubated for 3 h at 37°C in 5% CO_2, washed once with Casamino-DMEM (cDMEM [34]), and overlaid with a 100-μl substrate solution containing 1 μM CCF2/AM, 2.5 mM probenecid (Sigma), and 20 μl of 6× CCF2/AM loading solution (CCF2/AM loading kit, Invitrogen) diluted in cDMEM. Immediately after addition of the substrate solution, the plates were placed in a plate reader (SPECTRAFluor Plus; Tecan) set at 37°C. Cells were excited at 405 nm, and emission at 465 nm and 535 nm was recorded at 150-s intervals. The slopes of product accumulation over time for the interval of 20 to 40 min after the addition of substrate solution were calculated and represent effector-BlaM levels inside the HeLa cells.

Time-lapse-microscopy translocation assay. On day 1, HeLa cells were seeded in glass-bottom dishes (Matek) (uncoated, 35-mm diameter, coverslip no. 1) at a density of ~0.4 × 10^6 cells/dish in DMEM (Sigma) supplemented with 10% fetal calf serum (FCS) and antibiotics (Pen/Strep). In parallel, bacterial strains were inoculated into LB broth and grown overnight, at 37°C, as a static culture. On day 2, EPEC strains were diluted 1:100 with cDMEM supplemented with 2.5 mM probenecid (Sigma) and grown under conditions known to stimulate TTSS expression (growth at 37°C in 5% CO_2 for 2 h 45 min to an optical density at 600 nm [OD_{600}] of 0.2 to 0.35), creating a preactivated culture (34). An hour after growth of the bacterial cultures described above was started, HeLa cells were washed twice with cDMEM and treated with 240 μl of cDMEM containing 40 μl of 6× CCF2/AM loading solution (CCF2/AM loading kit, Invitrogen) (1 μM CCF2/AM and 2.5 mM probenecid). The cells were incubated for 60 min in the dark, at room temperature, followed by an additional 15 min at 37°C and then gently washed with 2 ml of cDMEM supplemented with 2.5 mM probenecid and infected with 2 ml of preactivated EPEC culture or a 1:50 dilution of *Salmonella* Typhimurium overnight culture in 2 ml of prewarmed cDMEM (40 μl in 2 ml) (MOI = ~40). Based on the optimization results (see Fig. S1 in the supplemental material), infection with *Salmonella* Typhimurium was carried out using an MOI of 40. However, due to the fact that adherent HeLa cells strictly localized to the bottom of the well whereas the bacteria were evenly distributed in the medium, the effective MOI was around 1. Immediately after infection, the dish was placed in a chamber on the microscope stage set at 37°C, and the infection process was recorded.

Time-lapse microscopy. Time-lapse movies were obtained at ×40 magnification (objective, Edmunds Optics [EC] Plan-Neofluar 40× 1.30 oil differential inference contrast [DIC]; Zeiss) with an automated, Zeiss Observer Z1 inverted fluorescence microscope and a monochromatic camera (AxioCam MRm rev. 3; Zeiss). The system was controlled by AxioVision REL 4.7 (Zeiss) software, which integrated time-lapse acquisition, stage motors, and a software-based autofocus motor. In each experiment, time-lapse movies were obtained from three fields of view. Each movie was taken at a time resolution of 60 or 90 s (*Salmonella* Typhimurium or EPEC, respectively). Each time point included three or four images: phase contrast and blue fluorescence (beta-lactamase set 1 [BM05685-1]; Chroma), green fluorescence (beta-lactamase set 2 [BM05685-2]; Chroma), and red fluorescence (Semrock BrightLine zero set for mCherry [mCherry-A-000-ZERO]; Chroma). Time-lapse movies were converted to an uncompressed AVI format using AxioVision REL 4.7 (Zeiss) software.

Image analysis of time-lapse movies. Prior to the movie conversion to AVI format, a flat-field correction was separately done to each captured channel using AxioVision REL 4.7 (Zeiss) software. We used a manual image analysis tool implemented in ImageJ 1.45 (NIH). All the captured images were subjected to image background correction (background subtraction). Regions of interest (ROIs) were chosen manually for each measured cell, and data corresponding to the mean intensity as a function of time in the blue and green channels were collected for each cell. Each data point [$P_{(t)}$] represents the division of green mean intensity [$P_{raw(t)}$] by the blue mean intensity [$S_{raw(t)}$] of the same time point calculated as follows: $[P_{(t)}] = [P_{raw(t)}]/[S_{raw(t)}]$.

SUPPLEMENTAL MATERIAL

Supplemental material for this article may be found at http://mbio.asm.org/lookup/suppl/doi:10.1128/mBio.00303-13/-/DCSupplemental.

Text S1, DOC file, 0.1 MB.
Figure S1, TIF file, 0.3 MB.
Figure S2, TIF file, 0.2 MB.
Figure S3, TIF file, 0.3 MB.
Figure S4, TIF file, 0.3 MB.
Movie S1, AVI file, 6.1 MB.
Movie S2, AVI file, 10.6 MB.
Movie S3, AVI file, 10.6 MB.
Movie S4, AVI file, 10.6 MB.
Movie S5, AVI file, 0.6 MB.

ACKNOWLEDGMENTS

We thank B. Kenny for providing pCVD-422-deltaTir and members of the Rosenshine group for fruitful discussions.

This work was supported by a grant from the Israel Science Foundation founded by the Israel Academy of Science and Humanities. E.M. is a Golda Meir Fellow. M.N. is grateful to the Azrieli Foundation for the award of an Azrieli Fellowship. I.R. is an Etta Rosensohn Professor of Bacteriology.

REFERENCES

1. **Vallance BA, Chan C, Robertson ML, Finlay BB.** 2002. Enteropathogenic and enterohemorrhagic Escherichia coli infections: emerging

themes in pathogenesis and prevention. Can. J. Gastroenterol. **16:** 771–778.
2. **Clarke SC, Haigh RD, Freestone PP, Williams PH.** 2003. Virulence of enteropathogenic *Escherichia coli*, a global pathogen. Clin. Microbiol. Rev. **16:**365–378.
3. **Wong AR, Pearson JS, Bright MD, Munera D, Robinson KS, Lee SF, Frankel G, Hartland EL.** 2011. Enteropathogenic and enterohaemorrhagic Escherichia coli: even more subversive elements. Mol. Microbiol. **80:**1420–1438.
4. **Chen HD, Frankel G.** 2005. Enteropathogenic *Escherichia coli*: unravelling pathogenesis. FEMS Microbiol. Rev. **29:**83–98.
5. **Yona-Nadler C, Umanski T, Aizawa S, Friedberg D, Rosenshine I.** 2003. Integration host factor (IHF) mediates repression of flagella in enteropathogenic and enterohaemorrhagic Escherichia coli. Microbiology **149:** 877–884.
6. **Mills E, Baruch K, Charpentier X, Kobi S, Rosenshine I.** 2008. Real-time analysis of effector translocation by the type III secretion system of enteropathogenic Escherichia coli. Cell Host Microbe **3:**104–113.
7. **Dean P, Kenny B.** 2009. The effector repertoire of enteropathogenic E. coli: ganging up on the host cell. Curr. Opin. Microbiol. **12:**101–109.
8. **Elliott SJ, Wainwright LA, McDaniel TK, Jarvis KG, Deng YK, Lai LC, McNamara BP, Donnenberg MS, Kaper JB.** 1998. The complete sequence of the locus of enterocyte effacement (LEE) from enteropathogenic Escherichia coli E2348/69. Mol. Microbiol. **28:**1–4.
9. **Josenhans C, Suerbaum S.** 2002. The role of motility as a virulence factor in bacteria. Int. J. Med. Microbiol. **291:**605–614.
10. **Haraga A, Ohlson MB, Miller SI.** 2008. Salmonellae interplay with host cells. Nat. Rev. Microbiol. **6:**53–66.
11. **Ghosh P.** 2004. Process of protein transport by the type III secretion system. Microbiol. Mol. Biol. Rev. **68:**771–795.
12. **Elliott SJ, O'Connell CB, Koutsouris A, Brinkley C, Donnenberg MS, Hecht G, Kaper JB.** 2002. A gene from the locus of enterocyte effacement that is required for enteropathogenic *Escherichia coli* to increase tight-junction permeability encodes a chaperone for EspF. Infect. Immun. **70:** 2271–2277.
13. **Abe A, de Grado M, Pfuetzner RA, Sánchez-Sanmartín C, Devinney R, Puente JL, Strynadka NC, Finlay BB.** 1999. Enteropathogenic *Escherichia coli* translocated intimin receptor, Tir, requires a specific chaperone for stable secretion. Mol. Microbiol. **33:**1162–1175.
14. **Creasey EA, Delahay RM, Bishop AA, Shaw RK, Kenny B, Knutton S, Frankel G.** 2003. CesT is a bivalent enteropathogenic *Escherichia coli* chaperone required for translocation of both Tir and map. Mol. Microbiol. **47:**209–221.
15. **Elliott SJ, Hutcheson SW, Dubois MS, Mellies JL, Wainwright LA, Batchelor M, Frankel G, Knutton S, Kaper JB.** 1999. Identification of CesT, a chaperone for the type III secretion of Tir in enteropathogenic *Escherichia coli*. Mol. Microbiol. **33:**1176–1189.
16. **García-Angulo VA, Deng W, Thomas NA, Finlay BB, Puente JL.** 2008. Regulation of expression and secretion of NleH, a new non-locus of enterocyte effacement-encoded effector in Citrobacter rodentium. J. Bacteriol. **190:**2388–2399.
17. **Thomas NA, Deng W, Puente JL, Frey EA, Yip CK, Strynadka NC, Finlay BB.** 2005. CesT is a multi-effector chaperone and recruitment factor required for the efficient type III secretion of both *LEE*- and non-*LEE*-encoded effectors of enteropathogenic *Escherichia coli*. Mol. Microbiol. **57:**1762–1779.
18. **Thomas NA, Deng W, Baker N, Puente J, Finlay BB.** 2007. Hierarchical delivery of an essential host colonization factor in enteropathogenic Escherichia coli. J. Biol. Chem. **282:**29634–29645.
19. **Schlumberger MC, Müller AJ, Ehrbar K, Winnen B, Duss I, Stecher B, Hardt WD.** 2005. Real-time imaging of type III secretion: *Salmonella* SipA injection into host cells. Proc. Natl. Acad. Sci. U. S. A. **102:**12548–12553.
20. **Patel JC, Galán JE.** 2005. Manipulation of the host actin cytoskeleton by salmonella—all in the name of entry. Curr. Opin. Microbiol. **8:**10–15.
21. **Deng W, Yu HB, de Hoog CL, Stoynov N, Li Y, Foster LJ, Finlay BB.** 2012. Quantitative proteomic analysis of type III secretome of enteropathogenic Escherichia coli reveals an expanded effector repertoire for attaching/effacing bacterial pathogens. Mol. Cell. Proteomics **11:**692–709.
22. **Kenny B, DeVinney R, Stein M, Reinscheid DJ, Frey EA, Finlay BB.** 1997. Enteropathogenic E. coli (EPEC) transfers its receptor for intimate adherence into mammalian cells. Cell **91:**511–520.
23. **Wang D, Roe AJ, McAteer S, Shipston MJ, Gally DL.** 2008. Hierarchal type III secretion of translocators and effectors from Escherichia coli O157:H7 requires the carboxy terminus of SepL that binds to Tir. Mol. Microbiol. **69:**1499–1512.
24. **Büttner D.** 2012. Protein export according to schedule: architecture, assembly, and regulation of type III secretion systems from plant- and animal-pathogenic bacteria. Microbiol. Mol. Biol. Rev. **76:**262–310.
25. **Charpentier X, Oswald E.** 2004. Identification of the secretion and translocation domain of the enteropathogenic and enterohemorrhagic Escherichia coli effector Cif, using TEM-1 beta-lactamase as a new fluorescence-based reporter. J. Bacteriol. **186:**5486–5495.
26. **Berger CN, Crepin VF, Baruch K, Mousnier A, Rosenshine I, Frankel G.** 2012. EspZ of enteropathogenic and enterohemorrhagic Escherichia coli regulates type III secretion system protein translocation. mBio **3:**e00317-12. doi: 10.1128/mBio.00317-12.
27. **Aroeti B, Friedman G, Zlotkin-Rivkin E, Donnenberg MS.** 2012. Retraction of enteropathogenic E. coli type IV pili promotes efficient host cell colonization, effector translocation and tight junction disruption. Gut Microbes **3:**267–271.
28. **Zahavi EE, Lieberman JA, Donnenberg MS, Nitzan M, Baruch K, Rosenshine I, Turner JR, Melamed-Book N, Feinstein N, Zlotkin-Rivkin E, Aroeti B.** 2011. Bundle-forming pilus retraction enhances enteropathogenic Escherichia coli infectivity. Mol. Biol. Cell **22:**2436–2447.
29. **Kubori T, Matsushima Y, Nakamura D, Uralil J, Lara-Tejero M, Sukhan A, Galán JE, Aizawa SI.** 1998. Supramolecular structure of the Salmonella typhimurium type III protein secretion system. Science **280:** 602–605.
30. **Daniell SJ, Takahashi N, Wilson R, Friedberg D, Rosenshine I, Booy FP, Shaw RK, Knutton S, Frankel G, Aizawa S.** 2001. The filamentous type III secretion translocon of enteropathogenic Escherichia coli. Cell. Microbiol. **3:**865–871.
31. **Wong AR, Clements A, Raymond B, Crepin VF, Frankel G.** 2012. The interplay between the Escherichia coli rho guanine nucleotide exchange factor effectors and the mammalian RhoGEF inhibitor EspH. mBio **3:**e00250-11. doi: 10.1128/mBio.00250-11.
32. **Jepson MA, Pellegrin S, Peto L, Banbury DN, Leard AD, Mellor H, Kenny B.** 2003. Synergistic roles for the map and Tir effector molecules in mediating uptake of enteropathogenic Escherichia coli (EPEC) into non-phagocytic cells. Cell. Microbiol. **5:**773–783.
33. **Tu X, Nisan I, Yona C, Hanski E, Rosenshine I.** 2003. EspH, a new cytoskeleton-modulating effector of enterohaemorrhagic and enteropathogenic Escherichia coli. Mol. Microbiol. **47:**595–606.
34. **Berdichevsky T, Friedberg D, Nadler C, Rokney A, Oppenheim A, Rosenshine I.** 2005. Ler is a negative autoregulator of the *LEE1* operon in enteropathogenic *Escherichia coli*. J. Bacteriol. **187:**349–357.